

Synaptic loss in behavioural variant frontotemporal dementia

revealed by [¹¹C]UCB-J PET

Maura Malpetti¹, P. Simon Jones¹, Thomas E. Cope^{1,2,3}, Negin Holland^{1,2}, Michelle Naessens¹,
Matthew A. Rouse³, George Savulich⁵, Tim D. Fryer^{1,4}, Young T. Hong^{1,4}, Selena Milicevic
Sephton^{1,4}, Franklin I. Aigbirhio^{1,4}, John T. O'Brien^{2,5#}, James B. Rowe^{1,2,3#}

1 Department of Clinical Neurosciences, University of Cambridge, Cambridge, UK

2 Cambridge University Hospitals NHS Foundation Trust, Cambridge, UK

3 Medical Research Council Cognition and Brain Sciences Unit, University of Cambridge, UK

4 Wolfson Brain Imaging Centre, University of Cambridge, Cambridge, UK

5 Department of Psychiatry, University of Cambridge, Cambridge, UK

Joint senior authors

Running head title: Synaptic PET in frontotemporal dementia

Corresponding Author:

Dr. Maura Malpetti
Department of Clinical Neurosciences
University of Cambridge
Herchel Smith Building, Forvie Site
Robinson Way, Cambridge Biomedical Campus
Cambridge CB2 0SZ
Email: mm2243@medschl.cam.ac.uk

Abstract

Synaptic loss is an early feature of neurodegenerative disease models, and is often severe in *post mortem* clinical studies, including frontotemporal dementia. Positron emission tomography (PET) imaging with radiotracers that bind to synaptic vesicle glycoprotein 2A enables quantification of synapses *in vivo*. This study used [¹¹C]UCB-J PET in people with behavioural variant frontotemporal dementia (bvFTD), testing the hypothesis that synaptic loss is severe and related to clinical severity. We performed a cross-sectional observational study of bvFTD, *versus* healthy controls, in which participants underwent neurological examination, neuropsychological assessment, magnetic resonance imaging (MRI) and [¹¹C]UCB-J PET. Patients were recruited from the Cambridge Centre for Frontotemporal Dementia at the University of Cambridge, and healthy volunteers from the UK National Institute for Health Research Join Dementia Research register. Eleven people with a clinical diagnosis of probable bvFTD and 25 age- and sex-matched healthy controls were included. All participants underwent dynamic [¹¹C]UCB-J PET imaging, structural MRI and a neuropsychological battery, including the Addenbrooke's cognitive examination (ACE-R), and INECO frontal screening (IFS). General linear models were used to compare [¹¹C]UCB-J binding potential maps between groups, and correlate synaptic density with cognitive performance and clinical features in patients. Group-comparison and correlation analyses were also performed using partial-volume corrected [¹¹C]UCB-J binding potential from regions of interest (ROIs). Patients with bvFTD showed severe synaptic loss compared to controls. In particular, [¹¹C]UCB-J binding was significantly reduced bilaterally in medial and dorsolateral frontal regions, inferior frontal gyri, anterior and posterior cingulate gyrus, insular cortex and medial temporal lobe. Synaptic loss in the left frontal and cingulate regions correlated significantly with cognitive impairments as assessed with ACE-R and IFS. Results from ROI-based analyses mirrored the voxel-wise results. In keeping with preclinical models, and human post mortem data, there is widespread frontotemporal loss of synapses in symptomatic bvFTD, in proportion to disease

severity. [^{11}C]UCB-J PET could support translational studies and experimental medicines strategies for new disease-modifying treatments for neurodegeneration.

Key words: frontotemporal dementia, synaptic loss, [^{11}C]UCB-J, positron emission tomography

Introduction

Frontotemporal dementia is a clinically and pathologically heterogeneous group of neurodegenerative conditions. Similar clinical phenotypes arise from different pathologies (Bang *et al.*, 2015; Olney *et al.*, 2017), including 3R or 4R tauopathy, and TDP-43 pathology. Despite this molecular heterogeneity, *post mortem* human studies (Lipton *et al.*, 2001; Clare *et al.*, 2010) and animal models (Yoshiyama *et al.*, 2007) suggest that the spectrum of frontotemporal dementia is characterised by early and severe synaptic loss, even preceding neuronal death and atrophy.

Our hypothesis was that in people with frontotemporal dementia, synaptic loss is severe and proportionate to clinical severity. Regionally specific and clinically relevant loss of synapses has been shown in the tauopathies of Alzheimer's disease (Chen *et al.*, 2018; Mecca *et al.*, 2020; Vanhaute *et al.*, 2020; Coomans *et al.*, 2021; O'Dell *et al.*, 2021), progressive supranuclear palsy and corticobasal degeneration (Holland *et al.*, 2020, 2021). TDP-43 related frontotemporal lobar degeneration is also associated with synaptic loss (Ni *et al.*, 2021; Riku *et al.*, 2021). For the behavioural variant of frontotemporal dementia (bvFTD), characterised by progressive personality and behaviour changes, and cognitive decline, including executive impairments (Piguet *et al.*, 2011; Rascovsky *et al.*, 2011), we propose that synaptic loss would be most prominent in frontotemporal regions.

Previous evidence for synaptic loss in frontotemporal dementia has been indirect, including reduced synaptic density in carriers of mutations associated with frontotemporal dementia (Malpetti *et al.*, 2021), abnormal synaptic markers in cerebrospinal fluid (Goetzl *et al.*, 2016; Van Der Ende *et al.*,

2020; Bergström *et al.*, 2021), and progressive frontotemporal hypometabolism that is disproportionate to atrophy, indicated by [¹⁸F]FDG PET (Diehl-Schmid *et al.*, 2007; Malpetti *et al.*, 2019; Bejanin *et al.*, 2020; see Chételat *et al.*, 2020 for review). Recently, new tools to quantify synaptic density *in vivo* have been developed, including radioligands that bind selectively to synaptic vesicle protein 2A (SV2A) as an assay of synaptic density (Finnema *et al.*, 2016; Heurling *et al.*, 2019). Synaptic density changes only slightly in mid- and later-life (Finnema *et al.*, 2016; Michiels *et al.*, 2021), providing a stable background against which to assess the effect of disease and disease-severity.

Here, we used PET with the SV2A radioligand [¹¹C]UCB-J to assess the regional distribution of synaptic loss in patients with a clinical diagnosis of probable bvFTD, compared to age- and sex-matched controls. Synaptic density was estimated using non-displaceable binding potential (BP_{ND}), a metric proportional to binding site density. In this context, if proven useful, [¹¹C]UCB-J PET could become an important tool for patient stratification and a surrogate endpoint in clinical trials and early interventions. PET measures for synaptic density would give additive and complementary information to fluid marker evidence, which do not elucidate *in vivo* spatial distributions of brain changes and may be less sensitive in prodromal stages. This allows to test the utility of [¹¹C]UCB-J as an *in vivo* marker for synaptic loss in frontotemporal dementia, irrespective of whether the underlying pathology is Tau or TDP-43. We predicted substantial synaptic loss in frontotemporal regions across all patients, and a correlation with clinical severity.

Materials and Methods

Participants

Eleven patients with a clinical diagnosis of probable bvFTD (Rascovsky *et al.*, 2011) were recruited from the Cambridge Centre for Frontotemporal Dementia at Cambridge University Hospitals NHS

Foundation Trust and the University of Cambridge. Twenty-five healthy volunteers were recruited from the UK National Institute for Health Research Join Dementia Research (JDR) register.

Participants were screened for exclusion criteria: current or recent history (within the last 5 years) of cancer, current use of the anti-convulsant medication levetiracetam (that binds to SV2A, the target of [¹¹C]UCB-J), history or MRI evidence of ischaemic or haemorrhagic stroke, any severe physical illness or co-morbidity that would limit the ability to fully and safely participate in the study, and any contraindications to MRI. Eligible volunteers underwent a clinical and neuropsychological assessment including the Mini-mental State Exam (MMSE), revised Addenbrooke's Cognitive Examination (ACE-R), INECO frontal screening (IFS), the Frontotemporal Dementia Rating Scale (FTD-RS), and the Clinical Dementia Rating Scale (CDR). Within 3 months, all participants underwent brain imaging with 3T MRI and PET scanning with [¹¹C]UCB-J ((R)-1-((3-(methyl-¹¹C)pyridin-4-yl)methyl)-4-(3,4,5-trifluorophenyl)pyrrolidin-2-one).

The research protocol was approved by the Cambridge Research Ethics Committee (18/EE/0059) and the Administration of Radioactive Substances Advisory Committee. All participants provided written informed consent in accordance with the Declaration of Helsinki.

Imaging acquisition and processing

Full details of the protocol for [¹¹C]UCB-J synthesis, data acquisition, image reconstruction and kinetic analysis have been published elsewhere (Holland *et al.*, 2020; Milicevic Sephton *et al.*, 2020; Malpetti *et al.*, 2021). In brief, dynamic PET data acquisition was performed on a GE SIGNA PET/MR (GE Healthcare, Waukesha, USA) for 90 minutes following [¹¹C]UCB-J injection, with attenuation correction including the use of a multi-subject atlas method (Burgos *et al.*, 2014) and improvements to the brain MRI coil component (Manavaki *et al.*, 2019). Each emission image series was aligned and rigidly registered to T1-weighted MRI acquired in the same session (TR=3.6

msec, TE=9.2 msec, 192 sagittal slices, in-plane voxel dimensions 0.55×0.55 mm (subsequently interpolated to 1.0×1.0 mm); slice thickness 1.0 mm).

For each subject a [¹¹C]UCB-J BP_{ND} map was determined from dynamic images corrected for partial volume effects at the voxel level using the iterative Yang method (Erlandsson *et al.*, 2012). BP_{ND} was calculated using a basis function implementation of the simplified reference tissue model, with centrum semiovale as the reference tissue (Rossano *et al.*, 2019). Each BP_{ND} map was warped to the ICBM 152 2009a asymmetric MR template using parameters from the spatial normalisation of the co-registered T1 MR image with Advanced Normalization Tools (ANTs; <http://www.picsl.upenn.edu/ANTS/>). For voxel-wise analyses, the spatially normalised [¹¹C]UCB-J BP_{ND} maps were spatially smoothed with a 10 mm full width at half maximum (FWHM) gaussian kernel prior to statistical analysis.

For regional analysis, we used the n30r83 Hammers atlas (<http://brain-development.org>) modified to include segmentation of brainstem and cerebellum, and non-rigidly registered to the T1-weighted MRI of each participant. Regions were multiplied by a binary grey matter mask constructed in Statistical Parametric Mapping (SPM12 v7771, Institute of Neurology, London, UK) based on a >50% probability map smoothed to PET spatial resolution, and geometric transfer matrix partial volume correction was applied to each image of the dynamic series (Rousset *et al.*, 1998). Regional BP_{ND} was determined with the same kinetic modeling approach and reference tissue as for the BP_{ND} maps.

Statistical analyses

Voxel-wise analyses were performed using SPM12. First, a two-sample t-test was performed to compare the bvFTD group to controls across the whole brain. Second, to test the association between synaptic density and clinical severity in people with bvFTD, voxel-wise general linear models were applied across all patients, including ACE-R and IFS scores as dependent variables in

separate models (for IFS, the analyses used 10 patients due to missing data). Similar models were applied to test for associations between [^{11}C]UCB-J BP_{ND}, age and symptom duration. All results were tested at an uncorrected voxel height threshold of $p < 0.001$ combined with a familywise error (FWE) corrected cluster threshold of $p < 0.05$; peak voxels in clusters that reached the conservative voxel-level familywise error threshold (FWE $p < 0.05$) are also indicated.

We performed complementary analyses on regions of interest, using R version 4.0.0 (R Core team 2020, <https://www.r-project.org/>) and JASP (JASP team: <https://jasp-stats.org/>). [^{11}C]UCB-J BP_{ND} values from regions of interest were aggregated into left and right frontal lobe, temporal lobe, parietal lobe, occipital lobe, cingulate cortex, and included in the analyses alongside insula cortex, hippocampus, amygdala, and thalamus. First, two-sample t-tests were performed in each region to compare the bvFTD group to controls. Across all brain regions, p-values from t-tests were corrected with false-discovery rate (FDR) correction, and Cohen's d effect sizes were calculated. As explorative analyses, we also performed two-sample t-tests on [^{11}C]UCB-J BP_{ND} values of bvFTD group *vs* controls considering smaller regions, obtained from the Hammers atlas with and without partial-volume correction. Second, Spearman's correlation analyses were performed to test the association between cognitive performance and [^{11}C]UCB-J BP_{ND} in cortical regions. In addition to the above frequentist statistics, we also present Bayesian analogous tests for regional effects (<https://osf.io/gny35/>), furnishing the strength of the evidence for the null *vs* alternate hypotheses.

Data Availability Statement

Anonymized data may be shared upon request to the corresponding or senior author from a qualified investigator for non-commercial use, subject to restrictions according to participant consent and data protection legislation.

Results

Descriptive statistics

Demographic and clinical features for the two groups are given in Table 1. The groups were similar in age and sex, with cognitive deficits among patients typical for bvFTD.

Voxel-wise group comparisons and correlations with cognitive scores

Single-subject [^{11}C]UCB-J BP_{ND} maps for individual patients and the average BP_{ND} map across all controls are reported in Figure 1. People with bvFTD showed mild (patient 1) to severe (patient 11) regional synaptic loss compared to controls.

At the FWE-corrected voxel-level threshold ($p < 0.05$), the two-sample t-test on [^{11}C]UCB-J BP_{ND} maps revealed synaptic loss in the bvFTD group compared to controls ($5.1 \leq t \leq 9.3$) in frontal, temporal, insula and cingulate cortex, bilaterally (Figure 2, panel A). Group differences were most pronounced in medial frontal and orbitofrontal cortex, superior frontal regions, inferior frontal gyrus, insula cortex, anterior and superior temporal lobe, and anterior cingulate cortex ($t \geq 6.4$).

For voxel-wise correlation analyses between [^{11}C]UCB-J BP_{ND} and cognition, ACE-R showed a strong positive association ($r \geq 0.8$; $6.3 \leq t \leq 6.8$, $p < 0.001$ uncorrected at the voxel level and $p < 0.05$ FWE-corrected at the cluster level) between cognition and [^{11}C]UCB-J BP_{ND} in the anterior cingulate gyrus bilaterally, in the left superior and middle frontal gyri, and the medial anterior temporal lobe (Figure 2, panel B). IFS scores correlated positively ($r \geq 0.8$; $7.9 \leq t \leq 9.9$, $p < 0.001$ uncorrected at voxel level and $p < 0.05$ FWE-corrected at cluster level) with [^{11}C]UCB-J BP_{ND} in the superior and middle frontal gyri bilaterally, left cingulate cortex and inferior frontal gyrus, and left superior parietal gyrus and anterior medial temporal lobe (Figure 2, panel C). Voxel-wise correlation analyses did not reveal significant associations between [^{11}C]UCB-J BP_{ND} , age and symptom duration ($p < 0.001$ uncorrected).

ROI-based group comparisons and correlations with cognitive scores

Group comparison results by two-sample t-tests in each region of interest are shown in Figure 3 and in more detail in Supplementary Table 1. bvFTD caused severe synaptic loss in frontal and temporal lobes bilaterally, with the right cingulate and insula cortex showing the most severe loss ($-6.9 \leq t \leq -5.6$; $-2.7 \leq \text{Cohen's } d \leq -2.2$). Results from explorative two-sample t-tests on sub-regions are reported in Supplemental Material, including partial-volume corrected (Supplementary Table 2) and uncorrected (Supplementary Table 3) regional BP_{ND} .

Considering cortical regions of interest, Spearman's correlation between partial-volume corrected [^{11}C]UCB-J BP_{ND} and ACE-R scores revealed strong positive associations in the left frontal lobe ($r=0.791$, $p = 0.002$, Figure 4A), cingulate cortex ($r=0.700$, $p = 0.008$, Figure 4C) and parietal lobe ($r=0.591$, $p = 0.028$, Figure 4E). Spearman correlation analyses with IFS scores showed positive associations with [^{11}C]UCB-J BP_{ND} in the same regions: the left frontal lobe ($r=0.754$, $p = 0.006$, Figure 4B), cingulate cortex ($r=0.620$, $p = 0.028$, Figure 4D) and parietal lobe ($r=0.632$, $p = 0.025$, Figure 4F). Similar results were obtained with regional BP_{ND} values without partial volume correction.

Bayesian correlation analyses indicated strong evidence for the associations between [^{11}C]UCB-J BP_{ND} and ACE-R scores in the left frontal lobe (Bayes Factor (BF) = 56.2), cingulate cortex (BF=10.7), with positive evidence in the parietal lobe (BF=3.9). Bayesian correlation analyses of IFS indicated strong evidence for positive correlation in the left frontal lobe (BF=23.4) but a lack of positive evidence for or against a correlation in the left cingulate cortex (BF=2.3) and parietal lobe (BF=0.8). In Supplementary Table 4, explorative frequentist and Bayesian correlation analyses of regional [^{11}C]UCB-J BP_{ND} with MMSE, ACE-R and IFS sub-scores, and FTD-RS are reported.

Discussion

This study confirms the hypothesis that people with a clinical diagnosis of bvFTD have severe and widespread synaptic loss over frontotemporal cortex, including cingulum and insula. The synaptic

density in frontal and cingulate regions as quantified with [^{11}C]UCB-J BP_{ND} correlates with patients' cognitive performance. [^{11}C]UCB-J BP_{ND} was not related to the estimated symptom duration or age, in line with previous evidence (Michiels *et al.*, 2021). These principal results were observed with and without partial volume correction, and using both voxel-wise and regional analysis. The loss of synapses detected by [^{11}C]UCB-J PET raises three points of particular importance.

First, the decline of synaptic health – including synaptic density and synaptic plasticity – will directly affect brain connectivity and learning. Synaptic mediation of neurophysiological connectivity underpins cognitive function, while synaptic plasticity is one of the major determinants of learning and memory in multiple cognitive systems. In Alzheimer's disease, synaptic loss is more closely related to cognitive impairment than tau burden, beta-amyloid burden or neuronal loss (Spires-Jones and Hyman, 2014). Such a preeminent relationship may also hold in frontotemporal dementia. The distinctive distribution of synaptic loss in bvFTD across frontotemporal, insula and cingulate cortex is consistent with the typical distribution of its molecular pathologies, and its neurocognitive and behavioural profile. In this study, all of our cases were symptomatic ($\text{CDR} \geq 1$), although we note that behavioural and cognitive changes can emerge in the presymptomatic and prodromal stages of bvFTD, many years before dementia and diagnosis (Rohrer *et al.*, 2015; Malpetti *et al.*, 2020; Staffaroni *et al.*, 2020); and synaptic loss has been identified in the presymptomatic stage of those with highly penetrant mutations such as C9orf72 expansions (Malpetti *et al.*, 2021). Early synaptic dysfunction in these regions may explain the subtle pre-symptomatic behavioural change and executive dysfunction. In addition, synaptic loss may determine the neurophysiological signatures of bvFTD as assayed by magnetoencephalography (Hughes *et al.*, 2018; Sami *et al.*, 2018; Adams *et al.*, 2021; Shaw *et al.*, 2021; Copet *et al.*, 2022) as in Alzheimer's disease (Coomans *et al.*, 2021).

Second, quantifying the degree and distribution of synaptic loss can enrich models of frontotemporal dementia pathogenesis, in preclinical and clinical settings. For example, in

preclinical tauopathy models, connectivity more than proximity has been shown to influence the spread of diverse toxic oligomeric tau species (Clavaguera *et al.*, 2009, 2013; de Calignon *et al.*, 2012; Iba *et al.*, 2013; Ahmed *et al.*, 2014; Mudher *et al.*, 2017). Several mechanisms have been demonstrated at the synapse by which such toxic oligomeric Tau can be transferred between neurons. The oligomeric tau is in turn synaptotoxic (Lasagna-Reeves *et al.*, 2011; Sydow *et al.*, 2011), and affects synaptic health even in the absence of cell death. In Alzheimer's disease, *in vivo* human PET and CSF studies recently demonstrated a strong association between tau pathology and reduced synaptic integrity (Vanhaute *et al.*, 2020; Casaletto *et al.*, 2021; Coomans *et al.*, 2021). In other clinical disorders caused by tau-mediated frontotemporal lobar degeneration, the tauopathy seems to be synaptotoxic (Holland *et al.*, 2021), whilst synaptic density and connectivity seem to confer vulnerability to molecular pathology (Cope *et al.*, 2018; Holland *et al.*, 2021). In preclinical models, [¹¹C]UCB-J may now be used in autoradiography or *in vivo* PET (Finnema *et al.*, 2016; Nabulsi *et al.*, 2016; Bertoglio *et al.*, 2020; Varnäs *et al.*, 2020; Thomsen *et al.*, 2021; Xiong *et al.*, 2021) to quantify synapse density, where it is highly correlated with better established markers such as synaptophysin (Finnema *et al.*, 2016). [¹¹C]UCB-J therefore offers a bridge between preclinical and clinical models, where quantitative whole-brain models of pathogenesis in dementia, including frontotemporal dementia, can be improved by the inclusion of synaptic density estimates in addition to structural connectivity (Raj *et al.*, 2012) and post-synaptic structural integrity (Mak *et al.*, 2021). In addition, it is possible that tau and TDP-43 mediated bvFTD have distinct spatiotemporal profiles of synaptic loss. This could be tested with studies using [¹¹C]UCB-J PET in preclinical models and people with genetically determined familial frontotemporal dementia (Van Der Ende *et al.*, 2020; Bergström *et al.*, 2021), or in due course by *post mortem* examination of those who have undergone PET. However, we suggest that synaptic loss is a mechanistic convergence point, present across diverse molecular pathologies.

Third, with a critical role for synaptic health in mediating between the molecular pathology and cognitive-physiological impairment of frontotemporal dementia, the ability to quantify the degree

and distribution of synaptic loss can enhance novel experimental medicine studies (Cope *et al.*, 2021). The degree and distribution of loss may be used either for stratification in inclusion or analytical stages of an early-phase clinical trial. It may also be considered as an intermediate marker of efficacy, particularly where the mechanisms of action of a drug is upstream of synaptic loss or is directly related to synaptic resilience and preservation.

[¹¹C]UCB-J is not the only potential marker of synaptic health in frontotemporal dementia, and related disorders. A previous study using [¹⁸F]UCB-H PET to assess synaptic loss did not identify a deficit in frontotemporal dementia *vs* controls, nor was there a difference between frontotemporal dementia and Alzheimer's disease (Salmon *et al.*, 2021). The lower specific binding of [¹⁸F]UCB-H compared to [¹¹C]UCB-J may have contributed to the null result. Results with the alternative ligand [¹⁸F]-SDM8/SynVest-1 have not been reported in frontotemporal dementia yet. Several studies have used [¹⁸F]FDG PET to assess brain metabolism and interpreted changes as a marker of synaptic loss. Such metabolic change is disproportionate to atrophy (Bejanin *et al.*, 2020), but is not a direct measure of synaptic density. The direct comparison between [¹¹C]UCB-J and [¹⁸F]FDG PET in Alzheimer's disease indicated a high correlation in medial temporal regions, but not elsewhere (Chen *et al.*, 2021): measures of synaptic loss and hypometabolism may therefore provide complementary information about the underlying pathophysiology. In addition to [¹⁸F]FDG and [¹¹C]UCB-J PET, synaptic function may be assessed by electro-/magneto-encephalography. For example, in Alzheimer's disease, tau burden ([¹⁸F]flortaucipir) and synaptic loss ([¹¹C]UCB-J) are both associated with changes in magnetoencephalography (Coomans *et al.*, 2021). Fluidic markers of synaptic health are also emerging, including pentraxins (Van Der Ende *et al.*, 2020), although these are currently largely confined to CSF-based rather than blood-based assays. In comparison to other techniques, [¹¹C]UCB-J PET has excellent reproducibility which is advantageous for longitudinal and interventional studies.

Our study has several limitations. We acknowledge the relatively small sample size. However, the expected effect size in frontotemporal dementia was large (Cohen's $d > 1$), and power was estimated

to be sufficient ($\beta > 0.8$ for $\alpha < 0.05$). Moreover, we found consensus across different analytic methods: voxel-wise and ROI-based analyses, BP_{ND} values determined from data with and without partial-volume correction. The Bayesian tests confirmed that we had sufficient precision (analogous to power in frequentist tests) to support the alternate hypotheses ($BFs > 3$) with strong evidence from the eleven patients. The convergence over these statistical approaches mitigates against inadequate power and sample-dependant biases on the estimation of group differences and imaging-cognition associations. The replication of these findings with larger and multicentre clinical cohorts will nonetheless represent an important step to establish the generalizability of our results, and utility for clinical trials. Recruitment was based on clinical diagnosis, rather than neuropathology or genetics, but the clinical diagnosis was re-confirmed at serial clinical visits and has high clinicopathological correlation with either FTLD-Tau or FTLD-TDP43. Given the novelty of the radiotracer, the cohort has been scanned recently (within 24 months of submission) meaning survival analyses and neuropathological confirmation are not yet possible. Future PET-to-autopsy studies will be needed to investigate the association between *in vivo* measures of synaptic density and neuropathology. Nonetheless, the concordance of partial-volume-corrected and non-corrected analyses already indicate that the synaptic loss we observe is not simply attributable to atrophy.

To conclude, our study confirms that bvFTD is associated with significant and widespread frontotemporal loss of synapses, in proportion to disease severity. We suggest that [^{11}C]UCB-J PET can facilitate the validation of preclinical models, inform models of human pathogenesis, and inform the design of new disease-modifying treatment strategies.

Acknowledgements

We thank our participant volunteers and their caregivers for their participation in this study, the radiographers and radiochemists at the Wolfson Brain Imaging Centre, the FTD research nurses and clinical fellows at the Cambridge Centre for Frontotemporal Dementia and Related Disorders for their invaluable support. We also thank UCB Pharma for providing the precursor for [¹¹C]UCB-J.

Funding

This study was co-funded by the Wellcome Trust (220258); Race Against Dementia Alzheimer's Research UK (ARUK-RADF2021A-010); the Cambridge University Centre for Parkinson-Plus (RG95450); the National Institute for Health Research (NIHR) Cambridge Biomedical Research Centre (BRC-1215-20014: the views expressed are those of the authors and not necessarily those of the NIHR or the Department of Health and Social Care); Medical Research Council (SUAG/051 G101400); and the Association of British Neurologists, Patrick Berthoud Charitable Trust (RG99368). For the purpose of open access, the author has applied a CC BY public copyright licence to any Author Accepted Manuscript version arising from this submission.

Competing interests

Unrelated to this work, JTO has received honoraria for work as DSMB chair or member for TauRx, Axon, Eisai and Novo Nordisk, and has acted as a consultant for Biogen and Roche, and has received research support from Alliance Medical and Merck. JBR is a non-remunerated trustee of the Guarantors of Brain, Darwin College and the PSP Association (UK). He provides consultancy to Asceneuron, UCB, Astex, Curasen, Wave, SVHealth, and has research grants from AZ-Medimmune, Janssen, and Lilly as industry partners in the Dementias Platform UK.

References

Adams NE, Hughes LE, Rouse MA, Phillips HN, Shaw AD, Murley AG, et al. GABAergic cortical network physiology in frontotemporal lobar degeneration. *Brain* 2021; 144: 2135–2145.

Ahmed Z, Cooper J, Murray TK, Garn K, McNaughton E, Clarke H, et al. A novel in vivo model of tau propagation with rapid and progressive neurofibrillary tangle pathology: The pattern of spread is determined by connectivity, not proximity. *Acta Neuropathol* 2014; 127: 667–683.

Bang J, Spina S, Miller BL. Frontotemporal dementia. *Lancet* 2015; 386: 1672–1682.

Bejanin A, Tammewar G, Marx G, Cobigo Y, Iaccarino L, Kornak J, et al. Longitudinal structural and metabolic changes in frontotemporal dementia. *Neurology* 2020; 95: e140–e154.

Bergström S, Öijerstedt L, Remnestål J, Olofsson J, Ullgren A, Seelaar H, et al. A panel of CSF proteins separates genetic frontotemporal dementia from presymptomatic mutation carriers □: a GENFI study. 2021; 4: 1–14.

Bertoglio D, Verhaeghe J, Miranda A, Kertesz I, Cybulska K, Korat Š, et al. Validation and noninvasive kinetic modeling of [11C]UCB-J PET imaging in mice. *J Cereb Blood Flow Metab* 2020; 40: 1351–1362.

Burgos N, Cardoso MJ, Thielemans K, Modat M, Pedemonte S, Dickson J, et al. Attenuation correction synthesis for hybrid PET-MR scanners: Application to brain studies. *IEEE Trans Med Imaging* 2014

de Calignon A, Polydoro M, Suárez-Calvet M, William C, Adamowicz DH, Kopeikina KJ, et al. Propagation of Tau Pathology in a Model of Early Alzheimer's Disease. *Neuron* 2012; 73: 685–697.

Casaletto KB, Zetterberg H, Blennow K, Brinkmalm A, Honer W, Schneider JA, et al. Tripartite Relationship Among Synaptic, Amyloid, and Tau Proteins. *Neurology* 2021; 97: e284–e297.

Chen MK, Mecca AP, Naganawa M, Finnema SJ, Toyonaga T, Lin SF, et al. Assessing Synaptic Density in Alzheimer Disease with Synaptic Vesicle Glycoprotein 2A Positron Emission

Tomographic Imaging. *JAMA Neurol* 2018; 75: 1215–1224.

Chen MK, Mecca AP, Naganawa M, Gallezot JD, Toyonaga T, Mondal J, et al. Comparison of [11C]UCB-J and [18F]FDG PET in Alzheimer’s disease: A tracer kinetic modeling study. *J Cereb Blood Flow Metab* 2021; 41: 2395–2409.

Chételat G, Arbizu J, Barthel H, Garibotto V, Law I, Morbelli S, et al. Amyloid-PET and 18F-FDG-PET in the diagnostic investigation of Alzheimer’s disease and other dementias. *Lancet Neurol* 2020; 19: 951–962.

Clare R, King VG, Wirenfeltdt M, Vinters H V. Synapse loss in dementias. *J Neurosci Res* 2010; 88: 2083–2090.

Clavaguera F, Akatsu H, Fraser G, Crowther RA, Frank S, Hench J, et al. Brain homogenates from human tauopathies induce tau inclusions in mouse brain. *Proc Natl Acad Sci U S A* 2013; 110: 9535–9540.

Clavaguera F, Bolmont T, Crowther RA, Abramowski D, Frank S, Probst A, et al. Transmission and spreading of tauopathy in transgenic mouse brain. *Nat Cell Biol* 2009; 11: 909–913.

Coomans EM, Schoonhoven DN, Tuncel H, Verfaillie SCJ, Wolters EE, Boellaard R, et al. In vivo tau pathology is associated with synaptic loss and altered synaptic function. *Alzheimers Res Ther* 2021; 13: 35.

Cope TE, Rittman T, Borchert RJ, Jones PS, Vatansever D, Allinson K, et al. Tau burden and the functional connectome in Alzheimer’s disease and progressive supranuclear palsy. *Brain* 2018; 141: 550–567.

Cope TE, Weil RS, Düzel E, Dickerson BC, Rowe JB. Advances in neuroimaging to support translational medicine in dementia. *J Neurol Neurosurg Psychiatry* 2021: 1–8.

Cope TE, Hughes LE, Phillips HN, Adams NE, Jafarian A, Nesbitt D, et al. Causal evidence for the multiple demand network in change detection: auditory mismatch magnetoencephalography across focal neurodegenerative diseases. *J. Neurosci.* in press (2022).

Diehl-Schmid J, Grimmer T, Drzezga a., Bornschein S, Riemenschneider M, Förstl H, et al.

Decline of cerebral glucose metabolism in frontotemporal dementia: a longitudinal 18F-FDG-PET-study. *Neurobiol Aging* 2007; 28: 42–50.

Van Der Ende EL, Xiao M, Xu D, Poos JM, Panman JL, Panman JL, et al. Neuronal pentraxin 2: A synapse-derived CSF biomarker in genetic frontotemporal dementia. *J Neurol Neurosurg Psychiatry* 2020; 91: 612–621.

Erlandsson K, Buvat I, Pretorius PH, Thomas BA, Hutton BF. A review of partial volume correction techniques for emission tomography and their applications in neurology, cardiology and oncology. *Phys Med Biol* 2012; 57

Finnema SJ, Nabulsi NB, Eid T, Detyniecki K, Lin SF, Chen MK, et al. Imaging synaptic density in the living human brain. *Sci Transl Med* 2016; 8: 1–10.

Goetzl EJ, Kapogiannis D, Schwartz JB, Lobach I V., Goetzl L, Abner EL, et al. Decreased synaptic proteins in neuronal exosomes of frontotemporal dementia and Alzheimer's disease. *FASEB J* 2016; 30: 4141–4148.

Heurling K, Ashton NJ, Leuzy A, Zimmer ER, Blennow K, Zetterberg H, et al. Synaptic vesicle protein 2A as a potential biomarker in synaptopathies. *Mol Cell Neurosci* 2019; 97: 34–42.

Holland N, Jones PS, Savulich G, Wiggins JK, Hong YT, Fryer TD, et al. Synaptic Loss in Primary Tauopathies Revealed by [11C]UCB-J Positron Emission Tomography. *Mov Disord* 2020; 35: 1834–1842.

Holland N, Malpetti M, Rittman T, Mak EE, Passamonti L, Kaalund SS, et al. Molecular pathology and synaptic loss in primary tauopathies: an 18F-AV-1451 and 11C-UCB-J PET study [Internet]. *Brain* 2021 Available from: <https://academic.oup.com/brain/advance-article/doi/10.1093/brain/awab282/6353021>

Hughes LE, Rittman T, Robbins TW, Rowe JB. Reorganization of cortical oscillatory dynamics underlying disinhibition in frontotemporal dementia. *Brain* 2018; 141: 2486–2499.

Iba M, Guo JL, McBride JD, Zhang B, Trojanowski JQ, Lee VMY. Synthetic tau fibrils mediate transmission of neurofibrillary tangles in a transgenic mouse model of alzheimer's-like tauopathy. *J Neurosci* 2013; 33: 1024–1037.

Lasagna-Reeves CA, Castillo-Carranza DL, Sengupta U, Clos AL, Jackson GR, Kaye R. Tau oligomers impair memory and induce synaptic and mitochondrial dysfunction in wild-type mice. *Mol Neurodegener* 2011; 6: 39.

Lipton AM, Munro Cullum C, Satumtira S, Sontag E, Hynan LS, White CL, et al. Contribution of asymmetric synapse loss to lateralizing clinical deficits in frontotemporal dementias. *Arch Neurol* 2001; 58: 1233–1239.

Mak E, Holland N, Jones PS, Savulich G, Low A, Malpetti M, et al. In vivo coupling of dendritic complexity with presynaptic density in primary tauopathies. *Neurobiol Aging* 2021; 101: 187–198.

Malpetti M, Carli G, Sala A, Cerami C, Marcone A, Iannaccone S, et al. Variant-specific vulnerability in metabolic connectivity and resting-state networks in behavioural variant of frontotemporal dementia. *Cortex* 2019; 120: 483–497.

Malpetti M, Holland N, Jones PS, Ye R, Cope TE, Fryer TD, et al. Synaptic density in carriers of C9orf72 mutations: a [11C]UCB-J PET study. *Ann Clin Transl Neurol* 2021; 8: 1515–1523.

Malpetti M, Jones PS, Tsvetanov KA, Rittman T, van Swieten JC, Borroni B, et al. Apathy in presymptomatic genetic frontotemporal dementia predicts cognitive decline and is driven by structural brain changes. *Alzheimer's Dement* 2020: 1–15.

Manavaki R, Hong Y, Fryer TD. Brain MRI coil attenuation map processing for the GE SIGNA PET/MR: Impact on PET image quantification and uniformity. *IEEE Nucl Sci Symp Med Imaging Conf Proceedings* 2019

Mecca AP, Chen MK, O'Dell RS, Naganawa M, Toyonaga T, Godek TA, et al. In vivo measurement of widespread synaptic loss in Alzheimer's disease with SV2A PET. *Alzheimer's Dement* 2020; 16: 974–982.

Michiels L, Delva A, van Aalst J, Ceccarini J, Vandenberghe W, Vandembulcke M, et al. Synaptic density in healthy human aging is not influenced by age or sex: a 11C-UCB-J PET study.

Neuroimage 2021; 232: 117877.

Milicevic Sephton S, Miklovicz T, Russell J, Doke A, Li L, Boros I. Automated radiosynthesis of [11C]UCB-J for imaging synaptic density by PET. J Label Compd Radiopharm 2020; In press.

Mudher A, Colin M, Dujardin S, Medina M, Dewachter I, Alavi Naini SM, et al. What is the evidence that tau pathology spreads through prion-like propagation? Acta Neuropathol Commun 2017; 5: 99.

Nabulsi NB, Mercier J, Holden D, Carr S, Najafzadeh S, Vandergeten MC, et al. Synthesis and preclinical evaluation of 11C-UCB-J as a PET tracer for imaging the synaptic vesicle glycoprotein 2A in the brain. J Nucl Med 2016; 57: 777–784.

Ni J, Ren Y, Su T, Zhou J, Fu C, Lu Y, et al. Loss of TDP-43 function underlies hippocampal and cortical synaptic deficits in TDP-43 proteinopathies. Mol Psychiatry 2021

O'Dell RS, Mecca AP, Chen MK, Naganawa M, Toyonaga T, Lu Y, et al. Association of A β deposition and regional synaptic density in early Alzheimer's disease: a PET imaging study with [11C]UCB-J. Alzheimer's Res Ther 2021; 13: 1–12.

Olney NT, Spina S, Miller BL. Frontotemporal Dementia. Neurol Clin 2017; 35: 339–374.

Piguet O, Hornberger M, Mioshi E, Hodges JR. Behavioural-variant frontotemporal dementia: diagnosis, clinical staging, and management. Lancet Neurol 2011; 10: 162–172.

Raj A, Kuceyeski A, Weiner M. A Network Diffusion Model of Disease Progression in Dementia. Neuron 2012; 73: 1204–1215.

Rascovsky K, Hodges JR, Knopman D, Mendez MF, Kramer JH, Neuhaus J, et al. Sensitivity of revised diagnostic criteria for the behavioural variant of frontotemporal dementia. Brain 2011; 134: 2456–2477.

Riku Y, Seilhean D, Duyckaerts C, Boluda S, Iguchi Y, Ishigaki S, et al. Pathway from tdp-43-

related pathology to neuronal dysfunction in amyotrophic lateral sclerosis and frontotemporal lobar degeneration. *Int J Mol Sci* 2021; 22

Rohrer JD, Nicholas JM, Cash DM, van Swieten J, Dopper E, Jiskoot L, et al. Presymptomatic cognitive and neuroanatomical changes in genetic frontotemporal dementia in the Genetic Frontotemporal dementia Initiative (GENFI) study: A cross-sectional analysis. *Lancet Neurol* 2015; 14: 253–262.

Rossano S, Toyonaga T, Finnema SJ, Naganawa M, Lu Y, Nabulsi N, et al. Assessment of a white matter reference region for 11C-UCB-J PET quantification. *J Cereb Blood Flow Metab* 2019

Rousset OG, Ma Y, Evans AC. Correction for partial volume effects in PET: Principle and validation. *J Nucl Med* 1998

Salmon E, Bahri MA, Plenevaux A, Becker G, Seret A, Delhaye E, et al. In vivo exploration of synaptic projections in frontotemporal dementia. *Sci Rep* 2021; 11: 16092.

Sami S, Williams N, Hughes LE, Cope TE, Rittman T, Coyle-Gilchrist ITS, et al.

Neurophysiological signatures of Alzheimer's disease and frontotemporal lobar degeneration: Pathology versus phenotype. *Brain* 2018; 141: 2500–2510.

Shaw AD, Hughes LE, Moran R, Coyle-Gilchrist I, Rittman T, Rowe JB. In vivo assay of cortical microcircuitry in frontotemporal dementia: A platform for experimental medicine studies. *Cereb Cortex* 2021; 31: 1837–1847.

Spires-Jones TL, Hyman BT. The Intersection of Amyloid Beta and Tau at Synapses in Alzheimer's Disease. *Neuron* 2014; 82: 756–771.

Staffaroni AM, Bajorek L, Casaletto KB, Cobigo Y, Goh SM, Wolf A, et al. Assessment of executive function declines in presymptomatic and mildly symptomatic familial frontotemporal dementia: NIH-EXAMINER as a potential clinical trial endpoint. *Alzheimer's Dement* 2020; 16: 11–21.

Sydow A, Van Der Jeugd A, Zheng F, Ahmed T, Balschun D, Petrova O, et al. Tau-induced defects

in synaptic plasticity, learning, and memory are reversible in transgenic mice after switching off the toxic tau mutant. *J Neurosci* 2011; 31: 2511–2525.

Thomsen MB, Jacobsen J, Lillethorup TP, Schacht AC, Simonsen M, Romero-Ramos M, et al. In vivo imaging of synaptic SV2A protein density in healthy and striatal-lesioned rats with [11C]UCB-J PET. *J Cereb Blood Flow Metab* 2021; 41: 819–830.

Vanhaute H, Ceccarini J, Michiels L, Koole M, Sunaert S, Lemmens R, et al. In vivo synaptic density loss is related to tau deposition in amnesic mild cognitive impairment. *Neurology* 2020; 95: e545–e553.

Varnäs K, Stepanov V, Halldin C. Autoradiographic mapping of synaptic vesicle glycoprotein 2A in non-human primate and human brain. *Synapse* 2020; 74: 1–6.

Xiong M, Roshanbin S, Rokka J, Schlein E, Ingelsson M, Sehlin D, et al. In vivo imaging of synaptic density with [11C]UCB-J PET in two mouse models of neurodegenerative disease. *Neuroimage* 2021; 239: 118302.

Yoshiyama Y, Higuchi M, Zhang B, Huang SM, Iwata N, Saido TCC, et al. Synapse Loss and Microglial Activation Precede Tangles in a P301S Tauopathy Mouse Model. *Neuron* 2007; 53: 337–351.

Tables

Table 1. Demographic and clinical characteristics for control and bvFTD groups. Mean and standard deviation are reported for each continuous variable. Group comparisons were performed with two-sample t-tests for continuous variables, and chi-square test for sex.

	Controls N=25	bvFTD N=11	<i>Difference</i>
Age	70.2 (7.0)	65.7 (9.3)	n.s.
Sex (F:M)	9:16	2:9	n.s.
MMSE [/30]	29.5 (1.1)	22.3 (8.6)	T(34)=2.8, p=0.019, d=1.2
ACE-R [/100]	96.2 (2.5)	63.0 (26.9)	T(34)=4.1, p=0.002, d=1.7
Att/Orient [/18]	17.9 (0.3)	13.0 (5.6)	T(34)=2.9, p=0.016, d=1.2
Memory [/26]	24.7 (1.7)	14.5 (8.4)	T(34)=4.0, p=0.002, d=1.7
Fluency [/14]	12.4 (1.5)	4.4 (4.5)	T(34)=5.8, p<0.001, d=2.4
Language [/26]	25.6 (0.8)	19.1 (7.6)	T(34)=2.8, p=0.018, d=1.2
Visuospatial [/16]	15.6 (0.6)	12.1 (4.0)	T(34)=2.9, p=0.015, d=1.2
IFS	25.7 (2.4)	9.4 (7.1)	T(32)=7.0, p<0.001, d=3.1
IFS WM	7.6 (1.3)	3.7 (2.4)	T(32)=5.0, p<0.001, d=2.1
Symptom duration (months)	-	79.9 (40.6)	-
FTD-RS %	-	18.9 (18.9)	-
FTD-RS Logit	-	-2.6 (1.7)	-

Abbreviations: bvFTD = behavioural variant frontotemporal dementia; MMSE = mini-mental state examination; ACE-R = Addenbrooke's cognitive examination revised; Att/orient = attention/orientation score; IFS = INECO frontal screening; WM = working memory; FTD-RS = frontotemporal dementia rating scale; ns = not significant; d = Cohen's d.

Figures

Figure 1. [^{11}C]UCB-J binding potential (BP_{ND}) maps for each bvFTD patient. The BP_{ND} maps were spatially normalised to ICBM 152 2009a space, masked and smoothed (isotropic 6mm full width at half maximum Gaussian for visualisation). The BP_{ND} maps are overlaid on the ICBM 152 2009a T1 MR template and the slices are reported in the neurological display convention (left on the left). For comparison, the first row on the left shows the corresponding average BP_{ND} map across 25 controls.

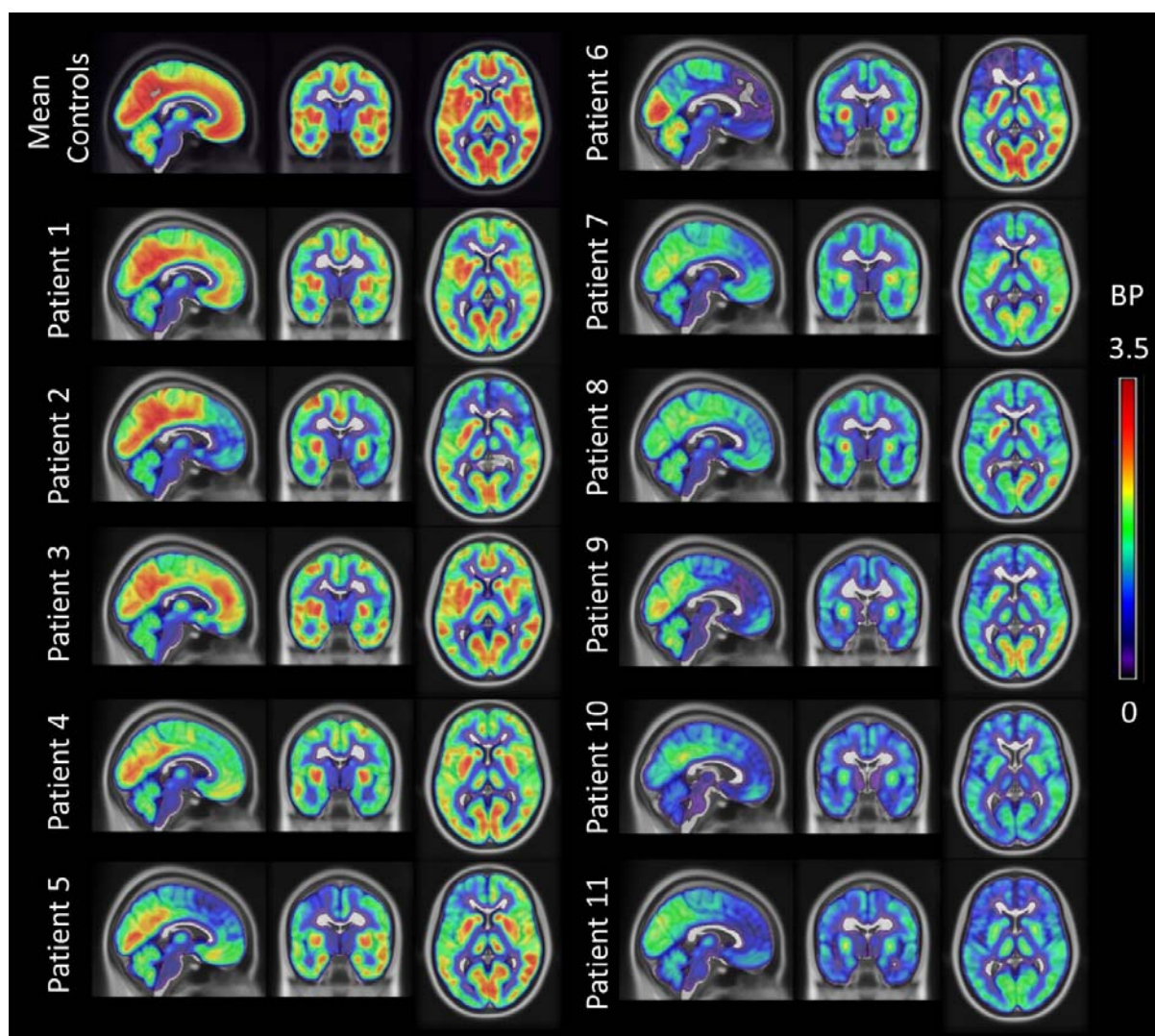


Figure 2. Voxel-wise synaptic loss and association with cognitive impairments in bvFTD. Panel

A: t maps from voxel-wise analysis showing higher [¹¹C]UCB-J binding potential in controls compared to bvFTD ($p < 0.05$ FWE-corrected at voxel level). Panels B and C: Coefficient of correlation maps for the bvFTD group between voxel-wise [¹¹C]UCB-J binding potential and cognitive performance at ACE-R and IFS ($p < 0.001$ uncorrected at voxel level, $p < 0.05$ FWE-corrected at cluster level).

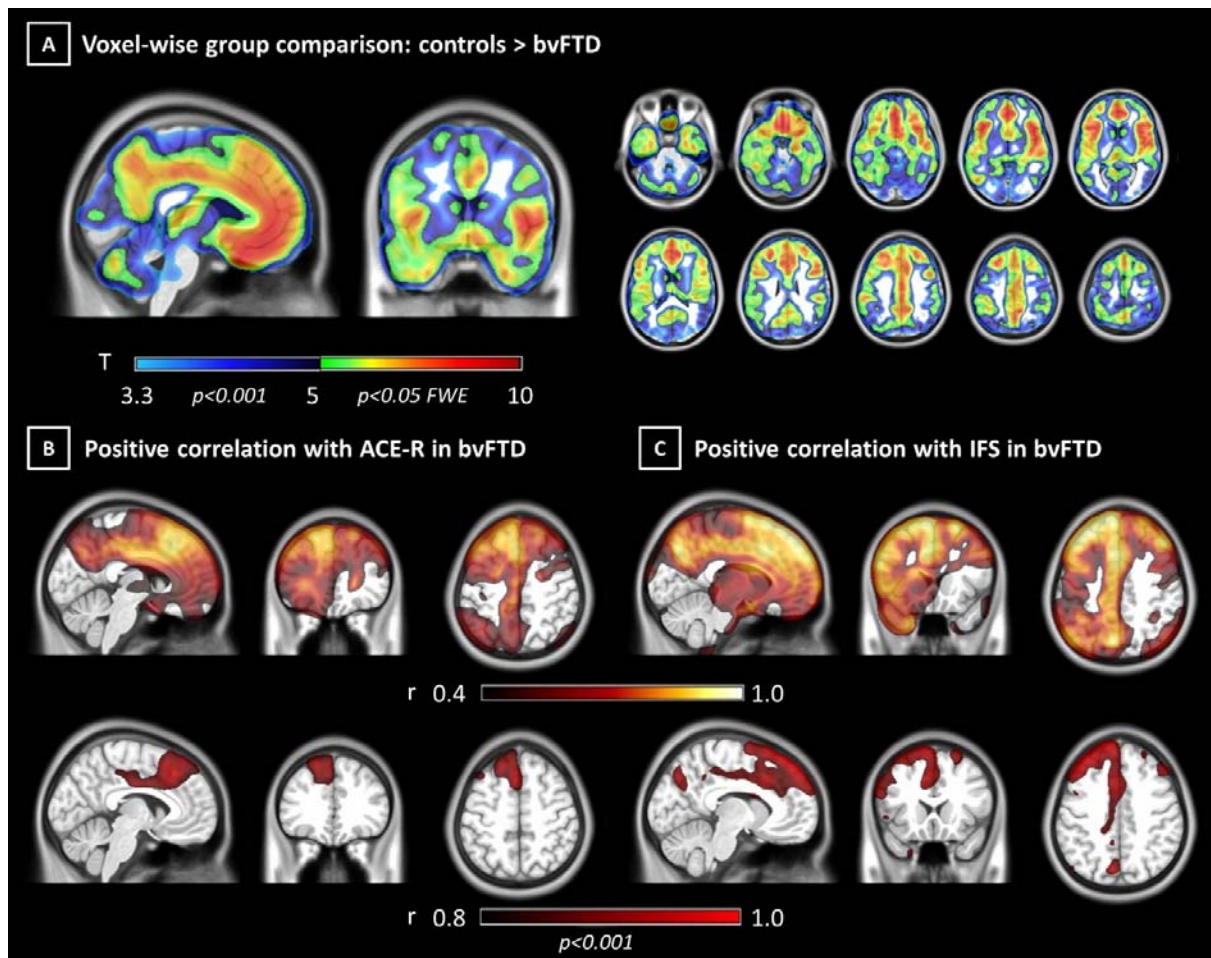


Figure 3. Regional partial-volume corrected binding potential (BP_{ND}) values and group

comparisons. Panel A: Regional [^{11}C]UCB-J BP_{ND} values for bvFTD patients (blue) and controls (grey). Panel B: Regional t values for comparison of [^{11}C]UCB-J BP_{ND} between bvFTD patients and controls ($p < 0.05$ FDR-corrected) surface rendered on. Panel C: For visual comparison with panel B, corresponding t-values obtained from voxel-wise group comparison.

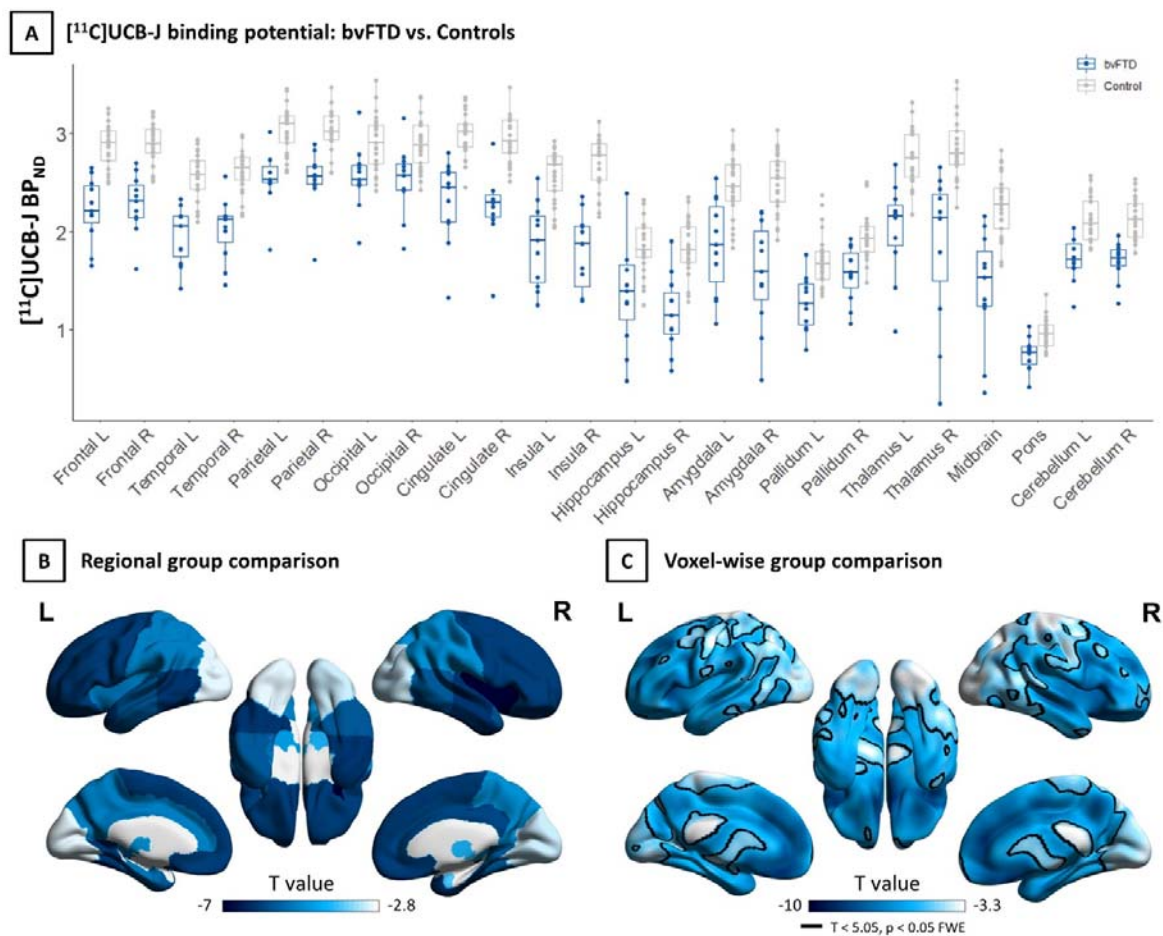


Figure 4. Correlations between regional synaptic density and cognitive performance.

[¹¹C]UCB-J binding potential in a cortical region is reported on the x axis, while the y axis represents a cognitive test score. Abbreviations: ACER = Addenbrooke's cognitive examination revised; BF = Bayes factor; IFS = INECO frontal screening; r = Spearman rho.

